Lira, Jorge
A Probabilistic Model to Quantify the Quality of Open Water Bodies
Geofísica internacional, vol. 59, no. 1, 2020, January-March, pp. 13-25
Instituto de Geofísica, UNAM

DOI: https://doi.org/10.22201/igeof.00167169p.2020.59.1.2077

Available in: https://www.redalyc.org/articulo.oa?id=56872303002

Geofísica Internacional (2020) 59-1: 13-25

Original paper

A Probabilistic Model to Quantify the Quality of Open Water Bodies

Jorge Lira

Received: August 13, 2018; accepted: November 14, 2019; published on line: January 6, 2020

Resumen

Se desarrolló un modelo para cuantificar la calidad de los cuerpos de agua abiertos sobre la base de la lógica probabilística multivariada. El modelo se basa en parámetros de calidad del agua que ya habían sido reportados en la literatura, tales como: turbidez, clorofila-a, índice de vegetación y usos de la temperatura superficial derivadas de la distribución de valores de píxeles de los parámetros. Dichas funciones se combinaron mediante la lógica probabilística multivariada que produjo un mapa de niveles de calidad del agua. Posteriormente, el modelo se aplicó a los humedales Centla, ubicados en el sureste de México. En ellos pueden observarse numerosos cuerpos de agua en niveles de eutrofización variables. Para probar el modelo propuesto, se desarrollaron ejemplos usando una imagen Terra/Aster. Además, se propuso una escala cualitativa de grados de calidad del agua.

Palabras clave: calidad del agua, lógica probabilística, parámetros del agua, humedales Centla

Abstract

A model to quantify the quality of open water bodies was developed on the grounds of multivariate probabilistic logic. The model is based on water quality parameters reported in the scientific literature such as: turbidity, chlorophyll-a, vegetation index and superficial temperature and uses probabilistic functions derived from the distribution of Pixel values of such parameters. Such functions were combined by means of the multivariate probabilistic logic that produced a map of water quality levels. The model was then applied to the Centla Wetlands in South East Mexico. In these wetlands, numerous water bodies can be observed in varying levels of eutrophication. To test the proposed model, examples were developed using a Terra/Aster image. A qualitative scale of water quality degrees was proposed.

Keywords: Water quality, Probabilistic logic, Water parameters, Centla Wetlands

Jorge Lira*
Instituto de Geofísica
Universidad Nacional Autónoma de México
Av. Universidad 3000
04510 Ciudad de México, México
**Corresponding author:jlira@geofisica.unam.mx*

I. Introduction

To define and quantify the quality of open water bodies many researchers in the field of environmental monitoring have utilised a number of parameters. For such quantification of water quality, several satellite-derived parameters were considered (Menken and Brezonik 2006; Philipson *et al.* 2016; Mushtaq and Lala 2017; Masocha *et al.* 2017). Various water quality parameters were derived using an airborne hyperspectral spectrometer (Koponen *et al.* 2002; Mobley *et al.* 2005). The most frequent parameters used are: chlorophyll-a, total suspended particles and transparency (Doña *et al.* 2014; Harvey *et al.* 2015). The transparency is determined by the Secchi disk depth (Song *et al.* 2011) and the suspended particles comprehend dead, inert and degraded organic matter (Reza 2008; Kilham at al. 2012; Yang *et al.* 2017). The transparency is inversely proportional to turbidity, the latter of which is determined by the absorption and scattering of light within a water column (Aguilar-Maldonado *et al.* 2017). The chlorophyll-a concentration is directly related to phytoplankton biomass and is used as an indicator for eutrophication (Menken and Brezonik 2006).

The Organization for Economic Co-operation and Development (OECD) defines eutrophication as the water enrichment in nutritive substances that generally leads to changes such as the increase in algae production and other aquatic plants, and the deterioration of water quality and aquatic ecosystem (Doña et al. 2014). The states of eutrophication are: ultraoligotrophic, oligotrophic, mesotrophic, eutrophic and hypertrophic. The water quality is inversely proportional to the degree of eutrophication.
Other water quality parameters, related to bio-chemical and thermodynamic processes in inland waters, were considered using vector regression and neural networks modelling with a limited sampling (Wang et al. 2011). The distribution of superficial temperature was also considered as an indicator of water quality (Korosov et al. 2007). For remote sensing studies of water quality using satellite images, only parameters with an optical response can be considered. A multivariate analysis of temperature, salinity and dissolved oxygen was performed using cluster analysis, principal component analysis and partial least square to assess the water quality of a coastal lagoon (Basatnia et al. 2018). The results indicated the critical need to monitor coastal water on a regular basis.

To retrieve water quality parameters from a multispectral satellite image, four different methods were applied (Campbell *et al.* 2011; Gholizadeh *et al.* 2016): (i) the look up table approach that compares the measured spectra response of optical water constituents with stored spectra; (ii) the neural network method that compares a large number of training data spectra to the measured spectra (Pozdnyakov *et al.* 2005a; El Din *et al.* 2017); (iii) the emPirical-regression that relates a linear combination of image bands with in-situ measurements (Bilge *et al.* 2003; Ficek *et al.* 2011; Lessels and Bishop 2013; Doña *et al.* 2014; Bonansea *et al.* 2015); (iv) the inversion/optimization method to simulate the spectra from a set of parameters that minimizes a cost function (Campbell *et al.* 2011). All four methods require a multispectral satellite image with adequate spatial and temporal resolution and in-situ measurements gathered close in time to the date of image acquisition.

A review article that accounts for space borne and airborne sensors used in the assessment of water quality was published in the scientific literature (Gholizadeh *et al.* 2016). The authors of the review included a comprehensive discussion of sensors and methods used in the evaluation of water quality parameters.

The research published accounts for the spatial and temporal variations of water quality parameters. However, a model that combines such parameters to produce a single output map dePicting varying levels of water quality is still required.

In this research a probabilistic model combining several water quality parameters is proposed. The water quality parameters considered are: Turbidity, Chlorophyll-a, Vegetation Index and Superficial Temperature. A model that considers such parameters and

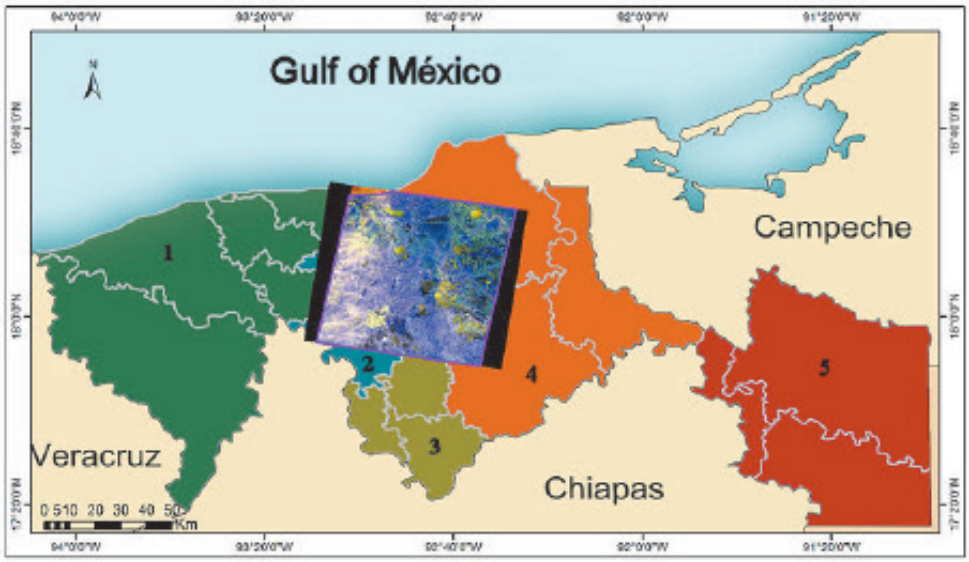

Figure 1. Area of study in Tabasco State, Southeast Mexico

produces a single image dePicting the degree of water quality is required. The model reported in this research combines such parameters using a procedure, based on fuzzy logic, and derived from multivariate probabilistic logic (Nilsson, 1986; Adams, 1996; Zalta *et al.* 2019). Multivariate probabilistic logic has been used in the past to produce maps of primary productivity (Lira *et al.*, 1992). An algorithm based on fuzzy logic was used to perform a multivariate fuzzy cluster analysis of open water bodies. Three clusters were obtained that represent three levels of water pollution (Wang and Wang 2009). These authors used hierarchical cluster analysis based on fuzzy cluster and multivariate statistical techniques. Such statistical techniques did not consider a multivariate probabilistic analysis. Rather, the authors employed sampling of water bodies to perform a classification of three levels of water pollution.

Details on the calculation of parameters are provided. A description of the basic principles of multivariate probabilistic logic and its application to model water quality are given. The area of study is the Centla Wetlands located in South East Mexico where numerous water bodies in varying degrees of eutrophication are observed

Table 1. Geophysical details of the subregions of Tabasco (location of the Centla Wetlands).

Subregion	Area (Ha)	Precipitation (mm)	Average height (masl)
Chontalpa	746,289	1,225	13.8
Centre	259,380	1,882	7.7
Sierra	184,727	3,711	24.7
Wetlands	663,568	1,225	1.7
Rivers	603,408	2,343	17.0

Ha - Hectares. masl - Metres above sea level

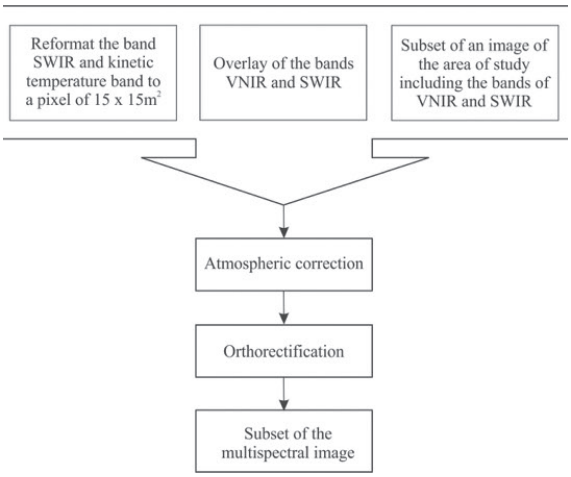

Figure 2. Block diagram of the preprocessing of the Terra/Aster image.

Table 2. Basic characteristics of the Terra/Aster multispectral image

Sensor	Date	Pixel size	Bands (□m)	Image size (pixels)
Terra/ Aster	March 13, 2001	Resampled to 15 x 15 m²	1) [0.52-0.60] 2) [0.63-0.69] 3) [0.76-0.86] 4) [1.60-1.70] 5) [2.145-2.185] 6) [2.185-2.225] 7) [2.235-2.285] 8) [2.295-2.365] 9) [2.360-2.430]	2.838 x 4,048

(Guerra-Martinez and Ochoa-Gaona 2006). An example is provided and a discussion of results is included.

II Materials and Methods

II.1 Materials

A wetland is a natural system defined as an extension of salt marshes, marshes, covered with water, regime natural or artificial, permanent or temporary, suspended or current, sweet or salty surfaces (Fondriest 2016). One important characteristic of the wetlands is that the substrate is periodically saturated or covered with water. Such saturation sustains the development of the ground and the communities of plants and animals that inhabit the wetlands.

The Centla Wetlands are located in the State of Tabasco to the South East of Mexico (Figure 1). The State of Tabasco is divided into five subregions: (1) Chontalpa, (2) Center, (3) Sierra, (4) Wetlands, (5) Rivers (Rodriguez 2002; Guerra-Martinez and Ochoa-Gaona 2006). The Centla Wetlands are included in the subregions (2) and (3) (Figure 1). The area covered by the satellite image is appreciated in Figure 1. Such image was overlaid over the subregions. Such overlay hinders the boundaries of the subregions. If such boundaries were shown in figure 1, the Centla water bodies would not be appreciated in its full extent.

A detailed description of the open water bodies that form the Centla Wetlands is included in the work by Rodriguez (2002). General morphologic and hydrologic conditions of the water bodies are included in such description. Table 1 provides basic geophysical details about the subregions. To develop the model proposed in this research, a Terra/Aster image was acquired (Table 2 and Figure 1).

II.2 Methods

II.2.1 Preprocessing of Terra/Aster Image

Bands 1 - 9 of the Terra/Aster image were resampled to a Pixel of 15 x 15 m², and geocoded to a UTM projection using the ephemeredes of the Terra/Aster Satellite (Table 2). An atmospheric correction was carried out using

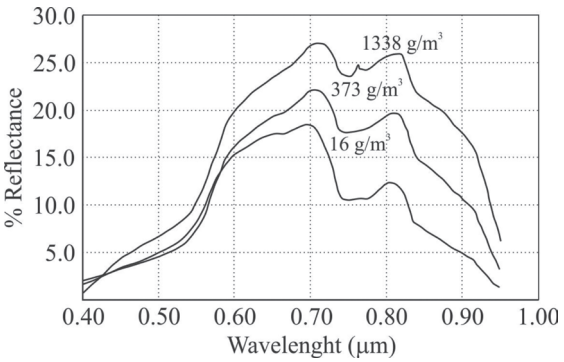

Figure 3. The reflectance of radiation as a function of the wavelength for several concentrations of suspended particles

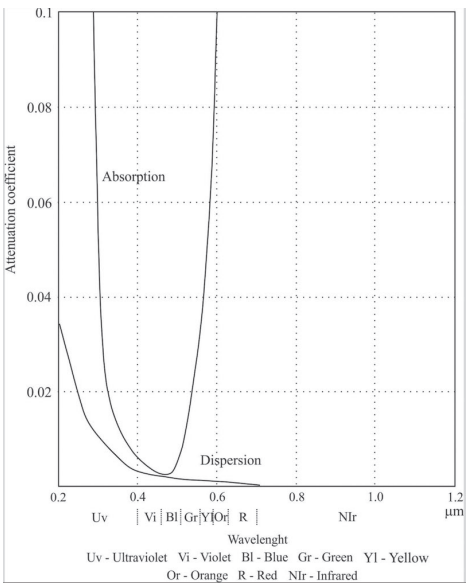

Figure 4. Attenuation of radiation as a result of scattering and absorption of radiation by suspended particles.

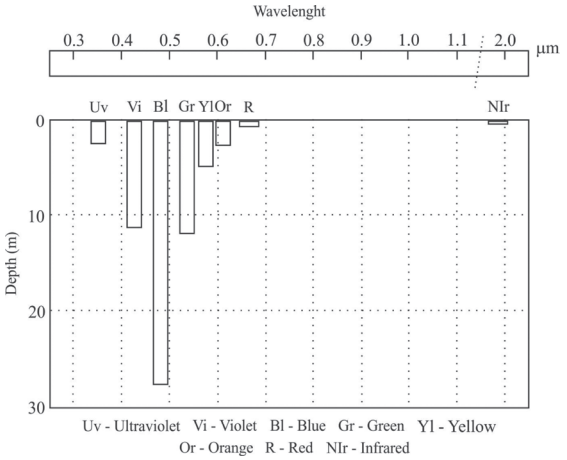

Figure 5. Depth of penetration of radiation as a function of wavelength in the optical region.

the method of dark object subtraction (Chavez 1996). A subimage was extracted to cover the area of the Centla Wetlands. The water bodies were segmented using a previous developed method (Lira 2006). The block diagram of Figure 2 dePicts the preprocessing of the image. The atmospheric correction was applied to the Visible and Near Infrared bands (VNIR) (bands 1-3) and Short Wave Infrared bands (SWIR) (bands 4-9) (Table 2). The kinetic band for the derivation of superficial temperature was acquired with atmospheric correction. The acquisition date of the Terra/Aster image is in line with field data reported by Rodriguez (2002).

II.2.2 Water Quality Parameters

The notion of water quality is used to describe the condition of a water body. This includes the chemical, physical and biological characteristics to quantify the degree to which water is useful with respect to its suitability for a particular purpose (Bartran and Ballance 1996). In this research the purpose is to determine the degree to which water is clean. Therefore, the parameters selected to quantify water quality of the water bodies in the study area are: Turbidity, Chlorophyll-a, Vegetation Index, and Temperature. These parameters were selected on the grounds of methods and results published in the scientific literature. The rational and calculation of these parameters is provided in the following sections.

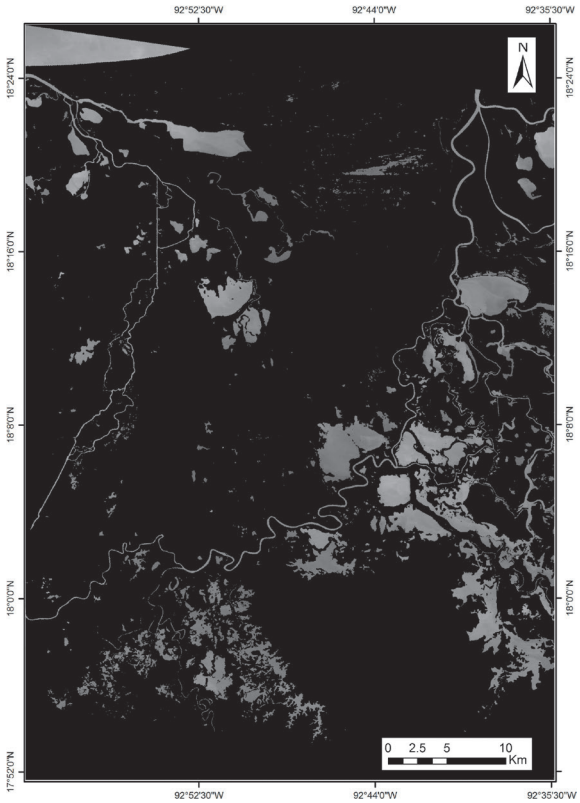

Figure 6. Turbidity map of the area of study.

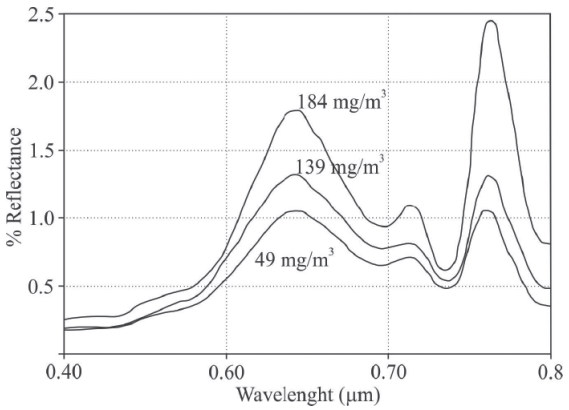

Figure 7. Spectra of Chlorophyll-a for several concentrations of this pigment.

Turbidity

The turbidity is used as a unit of measure to quantify the transmission of radiation through a column of water. Turbidity is defined as the degree of the haziness in water caused by suspended solids. The radiation is scattered and absorbed by the presence of suspended

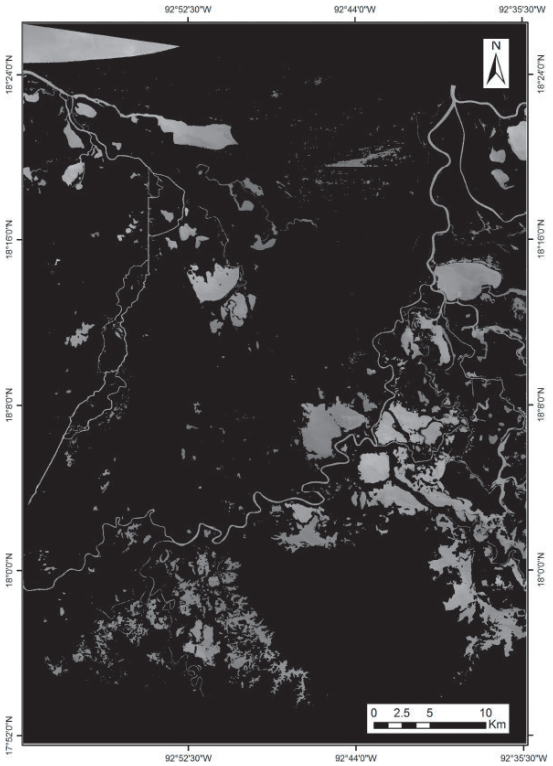

Figure 8. Chlorophyll-a map of the area of study.

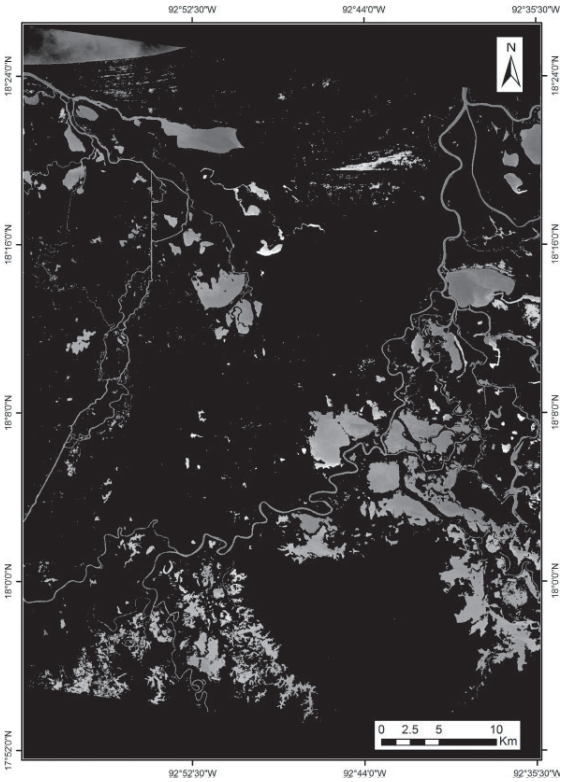

Figure 9. Vegetation index map of the area of study.

organic and inorganic particles in the water. The scattering of radiation increases as the density of suspended particles becomes higher (Roberts *et al.*, 1995) (Figure 3). The emPirical algorithms are derived from transfer radiation models that consider the spectral characteristics of suspended particles in the water (Ritchie *et al.* 2003). The scattering and absorption of radiation by suspended particles is a function of the wavelength (Bukata *et al.*, 1995) (Figure 4). The depth of penetration of radiation is a function of the wavelength (Bukata *et al.*, 1995) (Figure 5). The water bodies of the Centla Wetlands belong to Case II of inland waters (Pozdnyakov *et al.* 2005b). For this case, the model selected is

$$\text{Turbidity} = \frac{\text{Band}\,1 / \text{Band}\,2}{\text{Band}\,3 / \text{Band}\,2} \qquad (1)$$

The histogram of the image produced by equation (1) was elongated to a range of [0,255]. Figure 6 shows the Turbidity for the area of study.

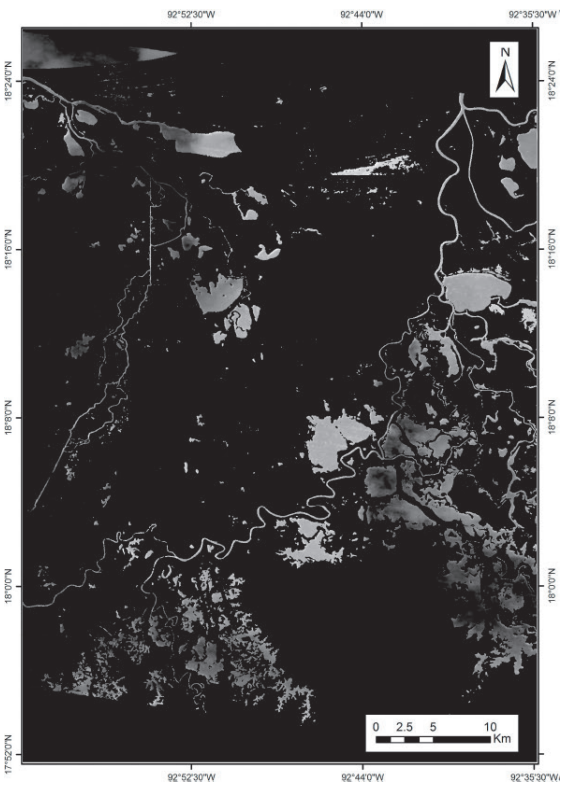

Figure 10. Superficial temperature map of the area of study.

Chlorophyll-a

The Chlorophyll-a is a photosynthetic Pigment. The concentration of Chlorophyll-a provides an indication of the volume of aquatic plants present in a water column. This Pigment is present in all groups of algae in coastal water bodies. The spectra for several concentrations of Chlorophyll-a shows a low reflectance in the bands corresponding to blue and red (Menken *et al.*, 2006) (Figure 7). Instead, in the bands of green and near infrared, a high reflectance is observed (Figure 7). On the grounds of the behaviour of such spectra (Doña *et al.*, 2014; Bonansea *et al.*, 2015), the model to calculate Chlorophyll-a is then

$$\text{Chlorophyll-a} = \frac{\text{Band}1}{\text{Band}2} \qquad (2)$$

The histogram of the image produced by equation (2) was elongated to a range of [0,255]. Figure 8 shows the Chlorophyll-a for the area of study.

Vegetation Index

Algae are plants that may affect water quality adversely by lowering the dissolved oxygen in the water. Some species of macrophytes in wetland areas can be detected by remote sensing. Species such as hydrilla and salvinia can be found in the area of study. In particular, salvinia is a floating plant in warm water bodies. The raPid growth rate of such plants can lead to a decrease in oxygen concentrations. The NDVI is used to estimate the presence of floating vegetation in the water bodies. The NDVI is defined as

$$\text{NDVI} = \frac{\text{Band}3 - \text{Band}2}{\text{Band}3 + \text{Band}2} \qquad (3)$$

The histogram of the image produced by equation (3) was elongated to a range of [0,255]. Figure 9 shows the Vegetation Index for the area of study.

Superficial Temperature

Temperature may be defined as a measurement of the average thermal energy of a substance. The solubility of oxygen and other gases will decrease as temperature increases. Therefore, an increase in temperature brings a decrease in water quality. The image of kinetic temperature was acquired from LP DAAC (Land Processes Distributed Active Archive Center) of NASA (National Aeronautics and Space Administration). This temperature image was generated from the five thermal bands (TIR); its original dimensions were 700 x 830 Pixels with a Pixel of 90 x 90 m^2. A reformat was applied to generate an image of the same size as the VNIR bands with a Pixel of 15 x 15 m^2. On the grounds of Planck law, the temperature emissivity algorithm was applied to the TIR bands. Such bands were previously corrected by atmospheric effects. The histogram of the image produced by the emissivity algorithm was elongated to a range of [0,255]. Figure 10 shows the Superficial Temperature for the area of study.

II.2.3 Multivariate Probabilistic Model

Nilsson (1986) first used the term probabilistic logic, where the truth-values of sentences are probabilities. The proposed semantical generalization induces a probabilistic logical entailment or logical consequence. If the probabilities of the argument premises are

Table 3. Matrix correlation among water quality indicators

	Chlorophyll-a	NDVI	Temperature	Turibidity
Chlorophyll-a	1.0000	-0.13327	-0.28643	0.74188
NDVI	-0.13327	1.0000	-0.28030	-0.38962
Temperature	-0.28643	0.28030	1.0000	-0.30620
Turbidity	0.74189	-0.38962	-0.30620	1.0000

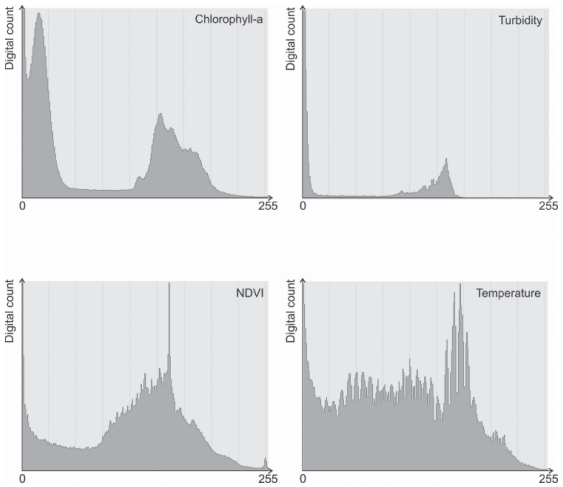

Figure 11. Histograms of the indicators used in the model of water quality.

known, then the probability of its conclusion may be derived (Adams 1996; Zalta *et al.* 2019). In this sense, the multivariate probabilistic model is based on the fact that probability functions can be assigned to logical sentences such as

P1 ==> Q, P2 ==> Q, . . ., Pn ==> Q (4)

These sentences read as follows: if indicator *Pi* exists, the natural process Q exists with a certain probability. Such probability is given by the density functions derived from indicator *Pi*. The implication *Pi* ==> Q, is a fuzzy set. If the value of the indicator *Pi* changes, the probability of the state of the natural process Q changes as well. In he multivariate probabilistic theory, the variables *Pi* are named indicators. In this research, the variables *Pi* are identified as the parameters described in Section II.2.2. The natural process Q is identified as the water quality. In the scientific literature, the physical quantities: Turbidity, Chlorophyll-a, NDVI and Superficial temperature are considered as parameters. The water quality is the variable that depends upon such parameters.

In an image, the value of indicator *Pi*, varies from one location to another, i.e., from Pixel to Pixel. A Pixel, defined as an elementary cell (k,l), implies that the logic sentence *Pi* ==> Q, is extended to every cell (k,l) where these are the coordinates of a Pixel in the image of a parameter.

Parameter Pi	Implication	Natural Processes Q
Turbidity	Increases	Water quality decreases
Chlorophyll-a	Increases	Water quality decreases
Vegetation index	Increases	Water quality decreases
Superficial temperature	Increases	Water quality decreases

Due to the fuzziness of the sentence *Pi* ==> Q, there is some degree of redundancy among indicators (Table 3). The correlation matrix (Table 3) indicates low correlation among the indicators. Therefore, the probability of the occurrence of Q should be evaluated when its

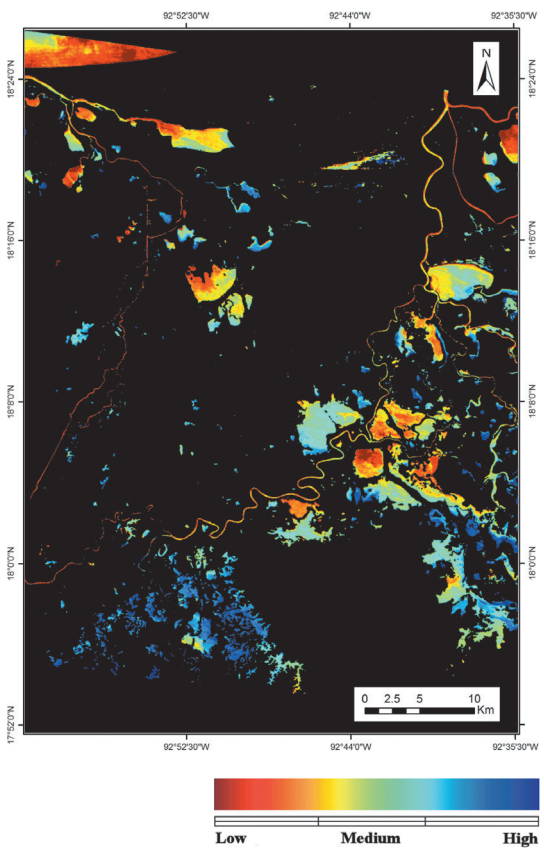

Figure 11. Thematic map of water quality in the area of study.

corresponding indicators occur simultaneously. For such evaluation we consider the intersection of every set determined by various indicators as

$$(P1 \cap P2 \cap P3 \cap ... Pn) ==> Q, \text{for every cell (k,l)} \quad (5)$$

The logical interpretation of this sentence is: if all indicators *Pi* occur simultaneously, the process Q can be calculated with some degree of probability. Equation (5) may be rewritten as

$$\bigcap_{i=1}^{n} (Pi \Rightarrow Q) \quad \text{, for every cell (k,l)} \quad (6)$$

Expression (6) is written explicitly as (Adams 1996; Zalta *et al.* 2019; Doménech et al, 2017)

$$1 - [- P1 \rightarrow Q)][1 - P2 \rightarrow Q)] \ldots [1 - Pn \rightarrow Q)] = \bigcap_{i=1}^{n} (Pi \Rightarrow Q) \quad (7)$$

Since *Pi* ==> Q are sets, equation (7) is equivalent to

$$\mathcal{P} = 1 - \prod_{i=1}^{n} (1 - Pi) \quad \text{, for every cell (k,1)} \quad (8)$$

The right term of equation (7) is the probability P of the occurrence of the process Q.

Since expression (8) is valid for every cell (k,l), the result is a spatial distribution of *P*. The result of *P* is an image where the probability of occurrence of Q is dePicted. The model (Expression 8) is dependent on the probability functions associated to the logic sentence *Pi* ==> Q. These functions must be modelled analytically or as tables supported by geophysical and biochemical principles and field data (Lira *et al.* 1992). In this research the probability functions are chosen as the density function associated to the Pixel values of each indicator. The histogram of the image parameters is a good approximation of the density functions (Figure 11). Since the histograms of image parameters are in the range [0,255], equation (8) is written as

$$\mathcal{P} = 255 - \prod_{i=1}^{n} (255 - Pi) \quad \text{, for every cell (k,1)} \quad (9)$$

The implication is that *Pi* ==> Q may have a direct or an inverse relationship. In this research an inverse relationship was determined. On the grounds of the discussion of Section II.2.2, the following set of implications describes the relationship of the parameters selected and the state of the natural processes Q.

In brief: if *Pi* increases ==> Q decreases.

Equation (9) was applied to the parameters selected in this research and the results are shown in Figure 12. The result of equation (9) is a map dePicted as an image in figure 12. The digital values of such image were assigned colors using a linear function. The color scale at the bottom of figure 12 is the visual representation of the relation digital value $\leftrightarrow$ color.

III. Results and Discussion

The four parameters calculated in this research for the generation of a water quality thematic map are dePicted in: figure 6 - Turbidity, figure 8 - Chlorophyll-a, figure 9 - Vegetation index, figure 10 - Superficial temperature. The histograms of indicators are in figure 11. The thematic map is shown in figure 12 and the discussion is divided according to such parameters. On the grounds of the definition of water quality used in this research (Bartran and Ballance 1996; Fondriest 2016), a qualitative colour code was associated to the thematic map. Such colour code dePicts the degree of water quality in the area of study of this research.

Turbidity

The North-West corner of the turbidity image shows a portion of the Gulf of Mexico. Due to the high concentration of sediments in the near-shore of the ocean, the turbidity is high (Figure 6). The water bodies with a connection to the ocean show a high level of turbidity as well. The rivers and canals located to the West and East show a high turbidity. A group of water bodies located to the Centre-East of the image has a high turbidity, whereas the water bodies to the South and Southeast are dePicted with low turbidity.

Chlorophyll-a

The Chlorophyll-a is high in the water bodies located to the Centre-East and Centre-South of the image (Figure 8). A high value is also observed in the near-shore ocean. An elongated body connected to the ocean shows a gradient of values for the whole set of parameters. A body in the centre of the image shows a high level of Chlorophyll-a. Other bodies located to the South-West show high values as well.

Vegetation index

Small bodies in the Centre-North and South-West are dePicted with high values of the vegetation index (Figure 9), while medium values are observed in the bodies to the South. The bodies connected to a river and to the ocean have a low value. Rivers and canals are observed with medium values. The near-shore ocean shows the lowest value.

Superficial temperature

The superficial temperature shows moderate values for medium size water bodies isolated from rivers or canals (Figure 10). The two large bodies located at the centre of the image appear as high temperature. A group of small bodies to the Centre-North have high temperature as well. The elongated body to the North, with connection to the ocean, appears with a gradient of temperature.

Thematic map

Figure 12 shows the thematic map derived from the model proposed in this research. A qualitative colour scale is included to indicate the levels of water quality. In general, isolated small water bodies have an appearance of high quality. The water bodies located to the South show medium and high quality, and the near-shore ocean and the water bodies connected to the sea appear with low water quality. Several bodies are dePicted with a gradient of water quality.

IV. Conclusions

Four parameters related to water quality published in the scientific literature, were calculated using a Terra/Aster image that includes the thermal band. The parameters were obtained on the grounds of well-known algorithms reported in several instances in the scientific literature. Such parameters were used in a multivariate probabilistic model to produce a thematic map of water quality for open water bodies. At present, water quality has been determined on the grounds of one parameter or several parameters but taken separately. The model suggested in this research, considers the joint use of the four most frequently reported parameters for water quality. A map is derived using equation (9). However, no quantitative scale yet has been defined. More work is required in this sense.

At present, no joint use of such parameters has been reported in the literature and no quantitative scale of water quality has been defined. The term water quality is usually employed with respect to its suitability for a particular purpose. In this research water quality is understood as the degree to which water is clean. A water is clean when it served the purpose of human consumption. Human consumption is understood in this work as water suitable for drinking ingestion and agricultural use. Thus, a high quality water body as derived in the present research may be considered as water adequate for human consumption. Therefore, a qualitative scale was associated to the colour-levels indicated in the water quality thematic map. Most of the water bodies show a gradient and a complex pattern of water quality. The water bodies to the South and Southeast exhibit a uniform degree of high water quality. All isolated water bodies appear with high values of water quality. The lowest quality observed was in the bodies that have some sort of connection to rivers and the ocean.

The map shown in figure 12 may be used to determine potential uses of the water for human consumption or agriculture. A good quality of the water is the most important asset to decision makers as discussed in the introduction.

A possible area of application of the model developed in this research may be the complex of lagoons in the area of TamPico-Altamira. The water of such lagoons is employed for human consumption; a critical decision must be made in this regard.

V. References

Adams, E.W., 1996. A primer of probability logic, CSLI Publication.

Aguilar-Maldonado, J.A., Santamaría-del-Ángel, E, Sebastiá-Frasquet. M.T.,2017, Reflectances of SPOT multispectral images associated with the turbidity of the Upper Gulf of California. *Revista de Teledección*, 50, 1 - 16.

Bartran J., Ballance R., 1996, Water quality monitoring - A practical guide to the design and implementation of freshwater quality studies and monitoring programmes. United Nations Environment Programme and the World Health Organization, Chapter 2, Water Quality.

Basatnia N., Hossein, S.A, Rodrigo-Comino J, Khaledian Y, Brevik E.C., Aitkenhead-Peterson J., Natesan U. , 2018, Assessment of temporal and spatial water quality in international Gomishan Lagoon, Iran, using multivariate analysis. *Environmental Monitoring and Assessment*, 19:314. /doi.org/10.1007/s10661-018-6679-2.

Bilge F, Yazici B, Dogeroglu T., Ayday C., 2003, Statistical evaluation of remotely sensed data for water quality monitoring. International Journal of Remote Sensing, 24, 5317 - 5326.

Bonansea M., Rodriguez M.C., Pinotti L., Ferrero S., 2015, Using multi-temporal Landsat imagery and linear mixing models for assessing water quality parameters in Río Tercero reservoir (Argentina). *Remote Sensing of Environment*, 158, 28 - 41.

Bukata R., Jerome J.H., Kondratyev K.Y., Pozdnyakov D.V., 1995, Optical properties and remote sensing of inland and coastal waters, New Cork: CRC Press.

Campbell G., Phinn S.R., Dekker A.G., Brando V.E., 2011, Remote sensing of water quality in an Australian troPical freshwater impoundment using matrix inversion and MERIS images. Remote Sensing of Environment, 115, 2402 - 2414.

Chavez Jr., P.S. ,1996, Image-based atmospheric corrections - Revisited and improved. Photogrammetric Engineering and Remote Sensing, 62, 1025–1036.

Doménech J.L.U., Nescolarde-Selva J.A., Segura-Abad L., 2017, Dialectical multivalued logic and probabilistic theory. Mathematics, 5, 15, doi:10.3390/math5010015.

Doña C., Sánchez J.M., Caselles V., Dominguez J.A., Camacho A., 2014 EmPirical relationships for monitoring water quality of lakes and reservoirs through multispectral images. IEEE Journal of Selected ToPics in Applied Earth Observations and Remote Sensing, 7, 632 - 1641.

El Din E.S., Zhang Y., Suliman A., 2017, MapPing concentrations of surface water quality parameters using a novel remote sensing and artificial intelligence framework. International Journal of Remote Sensing, 38, 1023 - 142.

Ficek D., Zapadka T., Dera J., 2011 Remote Sensing reflectance of Pomeranian Lakes and Baltic. Oceanología, 53, 959 - 970.

Fondriest Environmental, Inc., 2016, Fundamentals of Environmental Monitoring, Water quality. https://www.fondriest.com/environmental-measurements/parameters/water-quality/

Gholizadeh M.H., Melesse A.M., Reddi L., 2016, Spaceborne and airborne in water quality assessment. International Journal of Remote Sensing, 37, 3143 - 3180.

Guerra-Martinez V., Ochoa-Gaona S., 2006, Forest and land use assessment from 1990 to the year 2000 in Pantanos de Centla Biosphere Reserve, Tabasco, Mexico. Investigaciones Geográficas, Boletín del Instituto de Geografía, UNAM, 59, 7 - 25.

Harvey E.T., Kratzer S., Philipson P., 2015, Satellite-based quality monitoring for improved spatial and temporal retrieval of chlorophyll-a in coastal waters. Remote Sensing of Environment, 158, 417 - 430.

Kilham, N.E., Roberts D., Singer M.B., 2012, Remote sensing of suspended sediment concentrations during turbid flood conditions of the Feather River, California - A modeling approach. Water Resources Research, 48, W01521. doi:10.1029/2011WR010391

Koponen S., Pulliainen J., Kallio K., Hallikainen M., 2002, Lake water quality classification with airborne hyperspectral spectrometer and simulated MERIS data. Remote Sensing of Environment, 79, 51 -59.

Korosov A.A., Pozdnyakov D.V., Pettersson L.H., Grassl H., 2007, Satellite-data-based study of seasonal and spatial variations of water temperature and water quality parameters in Lake Ladoga. Journal of Applied Remote Sensing, 1, 011508.

Lessels J.S., Bishop T.F.A., 2013, Estimating water quality using linear mixed models with stream discharge and turbidity. Journal of Hydrology, 498, 13 - 22.

Lira, J., Marzolf, G.R., Marocchi, A., Naugle B., 1992, A probabilistic model to study spatial variations of primary productivity in river impoundments. Ecological Applications, 2, 86 - 94.

Lira J., 2006, Segmentation and morphology of open water bodies from multispectral images. International Journal of Remote Sensing, 27, 4015 - 4038.

Masocha M., Dube T., Nhiwatiwa T., Chomura D., 2017, Testing utility of Landsat 8 remote assessment of water quality in two subtroPical African reservoirs with contrasting trophic states. Geocarto International 2017. doi: 10.1080/10106049.2017.1289561.

Menken K.D., Brezonik P.L., 2006, Influence of Chlorophyll and colored dissolved organic matter (CDOM) on lake reflectance spectra: implications for measuring lake properties by remote sensing. Lake and Reservoir Management, 22, 179 - 190.

Mobley C.D., Sundman L.K., Davis C.O., Bowles J.H., Downes T.V., Leathers R.A., Montes M.J., Bissett W.P., Kohler D.D.R., Reid R.P., Louchard E.M., Gleason A., 2005, Interpretation of hyperspectral remote-sensing imagery by spectrum matching and look-up tables. Applied Optics, 44, 3576 - 3592.

Mushtaq F., Lala, M.G.N., 2017, Remote estimation of water quality parameters of Himalaya lake (Kshmir) using Landsat 8 OLI imagery. Geocarto International, 32, 274. 285.

Nilsson, N., 1986, Probabilistic logic. Artificial Intelligence, 28, 71 - 87.

Philipson P., Kratzer S., Mustapha S.B., Strömbeck N., Steler K., 2016, Satellite-based water quality monitoring in Lake Vänern Sweden. International Journal of Remote Sensing, 37, 3939 - 3960.

Pozdnyakov D., Korosov A., Grassl H., Pettersson L., 2005a, An advanced algorithm for operational retrieval of water quality from satellite data in the visible. International Journal of Remote Sensing, 26, 2669 - 2687.

Pozdnyakov D., Shuchman R., Korosov A., Hatt Ch., 2005b, Operational algorithm for the retrieval of water quality in the Great Lakes. Remote Sensing of Environment, 97, 352 - 370.

Reza M.M., 2008, Assessment of suspended sediments concentration in surface waters, using Modis images. American Journal of Applied Sciences, 5, 798 - 804.

Ritchie J., Zimba P., Everitt J., 2003, Remote sensing techniques to assess water quality. Photogrammetric Engineering and Remote Sensing, 69, 695 - 704.

Roberts A., Kirman C., Lesack L., 1995, Suspended sediment concentration estimation from multi-spectral video imagery. International Journal of Remote Sensing, 16, 2439 - 2455.

Rodriguez E., 2002, Las Lagunas Continentales de Tabasco. Universidad Juarez Autónoma de Tabasco, México.

Song K., Wang Z., Blackwell J., Zhang B., Li F., Zhang Y., Guangjia J., 2011, Water quality monitoring using Landsat Thematic Mapper data with emPirical algorithms in Chegan Lake, China. Journal of Applied Remote Sensing, 5, 053506-1 - 053506-16.

Wang, X., Wang, Q., 2009, Evaluation of landscape water bodies using fuzzy cluster and multivariate statistical techniques. Proceedings, IEEE International Conference on Intelligent Computing and Intelligent Systems, 20 - 22 November, 2009, Shangai, China, DOI: 10.1109/ICICISYS.2009.5357640.

Wang X., Fu L., He C., 2011, Applying support vector regression to water quality modeling by remote sensing data. International Journal of Remote Sensing, 23, 8615 - 8627.

Yang X., Sokoletsky L., Wei X., Shen F., 2017, Suspended sediment concentration mapPing based on the Modis satellite imagery in the East China inland, estuarine, and coastal waters. Journal of Oceanology and Limnology, 35, 39 - 60.

Zalta, E.N., Nodelman, U., Allen, C., Anderson, L. (Eds), 2019, Logic and Probability, The Stanford Encyclopedia of Philosophy, Stanford University, Stanford, CA, 94305, USA.